

1 **A sulfoglycolytic Entner-Doudoroff pathway in *Rhizobium leguminosarum* bv. *trifolii***

2 **SRDI565**

3

4

5 Jinling Li,<sup>1</sup> Ruwan Epa,<sup>1</sup> Nichollas E. Scott,<sup>3</sup> Dominic Skoneczny,<sup>4</sup> Mahima Sharma,<sup>5</sup>  
6 Alexander J.D. Snow,<sup>5</sup> James P. Lingford,<sup>2</sup> Ethan D. Goddard-Borger,<sup>2</sup> Gideon J. Davies,<sup>5</sup>  
7 Malcolm J. McConville,<sup>4</sup> Spencer J. Williams<sup>1\*</sup>

8

9

10 <sup>1</sup>School of Chemistry and Bio21 Molecular Science and Biotechnology Institute and  
11 University of Melbourne, Parkville, Victoria 3010, Australia

12

13 <sup>2</sup>ACRF Chemical Biology Division, The Walter and Eliza Hall Institute of Medical Research,  
14 Parkville, Victoria 3010, Australia and Department of Medical Biology, University of  
15 Melbourne, Parkville, Victoria 3010, Australia

16

17 <sup>3</sup> Department of Microbiology and Immunology, University of Melbourne at the Peter  
18 Doherty Institute for Infection and Immunity, Parkville, VIC, 3010, Australia

19

20 <sup>4</sup>Department of Biochemistry and Molecular Biology, Bio21 Molecular Science and  
21 Biotechnology Institute, University of Melbourne, Parkville, Victoria 3010, Australia

22

23 <sup>5</sup>York Structural Biology Laboratory, Department of Chemistry, University of York,  
24 Heslington YO10 5DD, United Kingdom

25

26 **Keywords**

27 Sulfoglycolysis; metabolomics; sulfur cycle; rhizobia; carbohydrates

28

29 E-mail: sjwill@unimelb.edu.au

30

31

32 **Abstract**

33 Rhizobia are nitrogen fixing bacteria that engage in symbiotic relationships with plant hosts  
34 but can also persist as free-living bacteria with the soil and rhizosphere. Here we show that  
35 free living *Rhizobium leguminosarum* SRDI565 can grow on the sulfosugar sulfoquinovose  
36 (SQ) using a sulfoglycolytic Entner-Doudoroff (sulfo-ED) pathway resulting in production of  
37 sulfolactate (SL) as the major metabolic end-product. Comparative proteomics supports the  
38 involvement of a sulfo-ED operon encoding an ABC transporter cassette, sulfo-ED enzymes  
39 and an SL exporter. Consistent with an oligotrophic lifestyle, proteomics data revealed little  
40 change in expression of the sulfo-ED proteins during growth on SQ versus mannitol, a result  
41 confirmed through biochemical assay of sulfoquinovosidase activity in cell lysates (data are  
42 available via ProteomeXchange with identifier PXD015822). Metabolomics analysis showed  
43 that growth on SQ involves gluconeogenesis to satisfy metabolic requirements for glucose-6-  
44 phosphate and fructose-6-phosphate. Metabolomics analysis also revealed the unexpected  
45 production of small amounts of sulfofructose and 2,3-dihydroxypropanesulfonate, which are  
46 proposed to arise from promiscuous activities of the glycolytic enzyme phosphoglucose  
47 isomerase and a non-specific aldehyde reductase, respectively. This work shows that  
48 rhizobial metabolism of the abundant sulfosugar SQ may contribute to persistence of the  
49 bacteria in the soil and to mobilization of sulfur in the pedosphere.

50

51 **Introduction**

52

53 Sulfur is essential for plant growth and is the fourth most important macronutrient after  
54 nitrogen, phosphorus, and potassium. Up to 10 kg/ha/y of sulfur is deposited in rain,  
55 especially near industrialized areas.<sup>1</sup> However, sulfur dioxide emissions from industrial  
56 sources have decreased in recent decades as a result of pollution mitigation and the move to  
57 low sulfur fuels and renewable energy sources, and quantities received from atmospheric  
58 sources is now at levels below that required by most crops.<sup>2</sup> Sulfur deficiency in soils is  
59 primarily combated by application of sulfur-containing fertilizers such as superphosphate,  
60 ammonium sulfate and gypsum,<sup>3</sup> which are applied across all major cropping and pasture  
61 areas worldwide.<sup>4</sup> Soils contain significant amount of sulfur, yet plants can only use sulfur in  
62 the form of sulfate and it has been shown that 95-98% of sulfur in soils is in the form of  
63 unavailable biological sulfur.<sup>4</sup> Thus, effective microbial cycling of sulfur from biological to  
64 inorganic forms within the soil is important<sup>5</sup> and has the potential to enhance crop yields and  
65 reduce reliance on fertilizers.

66 It is estimated that around 10 billion tonnes per annum of the sulfosugar  
67 sulfoquinovose (SQ) is produced annually by photosynthetic organisms, including plants,  
68 cyanobacteria and algae.<sup>6</sup> SQ is primarily found as the glycerolipid sulfoquinovosyl  
69 diacylglycerol (SQDG), and land plants can contain as much as 10% SQDG in their thylakoid  
70 membrane glycerolipids.<sup>7</sup> Very little is known about how SQ is metabolized within soils,  
71 although it has been shown to undergo very rapid mineralization to inorganic sulfate.<sup>8</sup> based  
72 on X-ray absorption near-edge spectroscopy measurements, it is estimated that 40% of sulfur  
73 within various sediments and humic substances exist as sulfonate.<sup>9</sup>

74 Bacteria are likely to be primarily responsible for the biomineralization of SQ,  
75 possibly by using SQ as a carbon source and catabolizing it via a modified version of  
76 glycolysis, termed sulfoglycolysis.<sup>10</sup> Two sulfoglycolytic processes have been described: the  
77 sulfoglycolytic Embden-Meyerhof-Parnas (sulfo-EMP) pathway,<sup>11</sup> and the sulfoglycolytic  
78 Entner-Doudoroff (sulfo-ED) pathway (Fig. 1).<sup>12</sup> The sulfo-ED pathway was first reported in  
79 *Pseudomonas putida* strain SQ1, a bacterium isolated from freshwater sediment, catabolised  
80 of SQ with excretion of equimolar amounts of sulfolactate (SL).<sup>12</sup> The sulfo-ED operon of *P.*  
81 *putida* SQ1 contains 10 genes including a transcriptional regulator, an SQ importer and SL  
82 exporter, a sulfoquinovosidase, SQ mutarotase, SQ dehydrogenase, SL lactonase, SG  
83 dehydratase, KDSG aldolase and SLA dehydrogenase enzymes. Based on genome-wide  
84 annotation studies, the sulfo-ED pathway is predicted to occur in a range of alpha-, beta- and

85 gamma-proteobacteria.<sup>12</sup> However, no direct evidence for this pathway has been reported for  
86 any organism other than *P. putida* SQ1. Other members of the microbial community can  
87 catabolize SL and 2,3-dihydroxypropanesulfonate (DHPS; the product of the sulfo-EMP  
88 pathway) to inorganic sulfur,<sup>13</sup> completing the biomineralization of SQ.

89 *Rhizobium leguminosarum* bv. *trifolii* SRDI565 (syn. N8-J), hereafter *Rl*-SRDI565,  
90 was isolated from a soil sample collected in western New South Wales but has the capacity to  
91 colonize *Trifolium subterraneum* subsp. *subterraneum* (subterranean clover) and other  
92 *Trifolium* spp.<sup>14</sup> Colonization of trifolium species with *Rl*-SRDI565 results in suboptimal  
93 nodulation and nitrogen fixation in some species and ineffective nitrogen fixation in others,  
94 leading to reduced shoot nitrogen content relative to other commercial strains.<sup>15</sup> Interestingly,  
95 the genome of *Rl*-SRDI565 encodes all the genes needed for a functional sulfo-ED  
96 pathway,<sup>16</sup> although there is no evidence to show that this is operative and/or that *Rl*-  
97 SRDI565 can use SQ as a major carbon source.

98 Rhizobia participate in sophisticated symbiotic relationships with leguminous host  
99 plants that allow them to fix atmospheric dinitrogen to provide a growth advantage to the  
100 host.<sup>17</sup> Symbiosis is triggered by molecular communication between the bacterium and the  
101 host resulting in nodule formation on the root and colonization by the bacterium. Within  
102 nodule bacteroids the energy intensive fixation of nitrogen is supported by C<sub>4</sub>-dicarboxylates  
103 (primarily malate, fumarate, and succinate) sourced from glycolysis of sucrose photosynthate  
104 within the plant host.<sup>17</sup> Owing to the importance of biological nitrogen fixation for input of  
105 nitrogen into the biosphere, the symbiosis of rhizobia and leguminous hosts has been well  
106 studied. However, rhizobia can also exist as free-living bacteria within the soil and  
107 rhizosphere.<sup>18</sup> Here, like other soil bacteria, they adopt a saprophytic and oligotrophic  
108 lifestyle where they utilize a variety of alternative carbon sources, including a wide range of  
109 carbohydrates.<sup>19</sup> Most likely, the ability of various rhizobia to persist in the pedosphere  
110 depends upon their ability to utilize diverse carbohydrate and non-carbohydrate substrates  
111 and establish an appropriate niche. SQ or its glycosides are likely to be a common soil  
112 constituent and nutrient given its ubiquitous production by plants. Possibly, the sulfo-ED  
113 pathway in *Rl*-SRDI565 might provide it with the capacity to survive on plant derived SQ or  
114 SQDG in the rhizosphere and in the soil.

115 Here we investigated whether the sulfo-ED pathway is active in *Rl*-SRDI565 and its  
116 potential role in utilizing plant-derived SQ or SQDG in the rhizosphere and in the soil. We  
117 show that *Rl*-SRDI565 can grow on SQ and sulfoquinovosyl glycerol (SQGro) as sole carbon  
118 source. Growth on SQ leads to excretion of SL into the growth media indicating active

119 sulfoglycolysis. This was supported by proteomic analyses, which showed that several genes  
120 in the sulfo-ED operon are upregulated when bacteria are grown on SQ, while metabolomic  
121 analyses confirm the presence of characteristic intermediates of the sulfo-ED pathway, as  
122 well as the unexpected production of intracellular DHPS. Overall, we show that *Rl*-SRDI565  
123 has an active pathway for SQ utilization which may support growth of this bacterium in the  
124 environment, and in turn provides a new model organism for the study of the sulfo-ED  
125 pathway.

126

127

128 **Results**

129 Analysis of the genome of *Rl*-SRDI565 revealed a sulfo-ED operon that had the same  
130 genes, but no synteny with the *P. putida* SQ1 operon (Figure 1). Genes with high sequence  
131 identity to the *P. putida* proteins included a putative SQase, SQ dehydrogenase, SL lactonase,  
132 SG dehydratase, KDSG aldolase and SLA dehydrogenase, and an SL exporter (see Figures  
133 S1-S6). The *Rl*-SRDI565 operon contains some important differences compared to that of *P.*  
134 *putida* SQ1. In particular, it lacks a putative SQ mutarotase,<sup>20</sup> and appears to use an ABC  
135 transporter cassette to import SQ/SQGro in place of an SQ/SQGro importer/permease. The  
136 putative sulfo-ED pathway in *Rl*-SRDI565 is consistent with the proposed protein functions  
137 outlined in Figure 1b, with a comparison to the classical ED pathway in Figure 1c.

138 Initial attempts were made to grow *Rl*-SRDI565 in completely defined medium, such  
139 as M9 minimal media containing 125 µg mL<sup>-1</sup> biotin<sup>21</sup>, to allow assessment of different  
140 carbon sources on bacterial growth. However, optimal growth could only be achieved using a  
141 yeast extract-based medium<sup>15</sup>. In particular robust growth was achieved using a 5% dilution  
142 of 1 g L<sup>-1</sup> yeast extract (Y<sub>5%</sub> media) containing 5 mmol mannitol (Y<sub>5%</sub>M), while no  
143 detectable bacterial growth was observed on Y<sub>5%</sub> media alone. Significantly, *Rl*-SRDI565  
144 also grew robustly on Y<sub>5%</sub> media containing 5 mM SQ (Y<sub>5%</sub>SQ) and reached the same final  
145 OD<sub>600</sub> value as in Y<sub>5%</sub>M (Figure 2a). *Rl*-SRDI565 also grew on Y<sub>5%</sub> media containing  
146 glucose, although to a lower final OD<sub>600</sub> than in Y<sub>5%</sub>M or Y<sub>5%</sub>SQ. <sup>13</sup>C NMR spectroscopic  
147 analysis of the culture media of stationary phase *Rl*-SRDI565 grown in Y<sub>5%</sub>SQ revealed the  
148 presence of three major signals corresponding to SL (Figure 2b). A fourth signal was also  
149 observed but not assigned and was also present in stationary phase media of cells grown on  
150 Y<sub>5%</sub>M, suggesting it is derived from other carbon sources in the yeast extract. *Rl*-SRDI565  
151 also grew on Y<sub>5%</sub> containing SQGro, but less robustly than on SQ.

152 We next examined changes in the proteome of *Rl*-SRDI565 cultivated on mannitol  
153 versus SQ. Label-free based quantitative proteomic analysis of five experimental replicates  
154 of *Rl*-SRDI565 cultivated on each carbon source, identified 2954 proteins, with 1943 proteins  
155 quantified in at least 3 experimental replicates under each growth condition (Supplementary  
156 Table 1). Expression levels of 30 proteins potentially associated with SQ metabolism were  
157 significantly elevated (-log<sub>10</sub>(p)>2 and a fold change greater than 2 log<sub>2</sub> units) in bacteria  
158 cultivated in Y<sub>5%</sub>SQ (Figures 3a and b). In particular, a suspected KDSG aldolase (annotated  
159 as alpha-dehydro-beta-deoxy-D-glucarate aldolase, WP\_017967308.1), a member of the  
160 proposed sulfo-ED pathway, was significantly increased (-log<sub>10</sub>(p)= 4.74429 and a fold

161 change of 2.38 log<sub>2</sub>). Consistent with the involvement of this pathway we also observed a  
162 significant yet less dramatic increase in the proposed SQase (annotated alpha-glucosidase,  
163 WP\_017967311.1) (-log<sub>10</sub>(p)= 1.43643 and a fold change of 1.02 log<sub>2</sub>). Additional members  
164 of the predicted pathway expressed at higher levels in SQ-fed bacteria included the suspected  
165 SQ dehydrogenase (annotated as SDR family oxidoreductase, WP\_017967310.1) identified  
166 by MS/MS events in 4 out of 6 SQ experiments compared to 1 mannitol experiment and the  
167 suspected SG dehydratase (annotated as dihydroxy-acid dehydratase, WP\_017967307.1)  
168 identified by MS/MS events in 3 out of 6 SQ experiments compared to 0 mannitol  
169 experiments (Figure S7). However, owing to their low abundance they could not be  
170 accurately quantified (Figure S8).

171 Other proteins that were significantly increased in SQ-fed bacteria included a  
172 NAD(P)-dependent oxidoreductase (WP\_017965793.1), NADH-quinone oxidoreductase  
173 subunit NuoH (WP\_017963854.1), a NAD-dependent succinate-semialdehyde  
174 dehydrogenase (WP\_017967313.1) and a citrate synthase/methylcitrate synthase  
175 (WP\_017964386.1) supporting an alteration with the TCA cycle and oxidative  
176 phosphorylation under conditions of growth on SQ (Figure 3b).

177 To demonstrate activity for a representative sulfo-ED enzyme from *Rl*-SRDI565, we  
178 cloned and expressed the gene encoding the putative SQase. To support future structural  
179 studies, we expressed the N-terminal hexahistidine tagged K375A/K376A variant, termed  
180 *Rl*SQase\*, a mutant enzyme whose design was guided by the Surface Entropy Reduction  
181 prediction (SERp) server (Figure S9).<sup>22</sup> Size exclusion chromatography-multiple angle light  
182 scattering (SEC-MALS) analysis of *Rl*SQase\* revealed that the protein exists as a dimer in  
183 solution (Figure S10). Enzyme kinetics were performed using the chromogenic SQase  
184 substrate 4-nitrophenyl  $\alpha$ -sulfoquinovoside (PNPSQ). *Rl*SQase\* exhibited a bell-shaped pH  
185 profile with optimum at pH 7-8 and consistent with titration of catalytically important  
186 residues of pKa1 = 6.5 ± 0.4 and pKa2 = 8.6 ± 0.3. The enzyme displayed saturation kinetics  
187 with Michaelis-Menten parameters  $k_{cat} = 1.08 \pm 0.17 \text{ s}^{-1}$ ,  $K_M = 0.68 \pm 0.25 \text{ mM}$ , and  $k_{cat}/K_M =$   
188  $1.59 \pm 0.83 \text{ s}^{-1} \text{ mM}^{-1}$  (Figure 4a and 4b).

189 Direct evidence for enzymatic activity associated with the sulfo-ED operon in *Rl*-  
190 SRDI565 was obtained by measuring SQase enzyme activity in cell lysates. The chromogenic  
191 substrate 4-nitrophenyl  $\alpha$ -sulfoquinovoside (PNPSQ), which was designed as an analogue of  
192 the natural substrate SQGro, results in release of the chromophore 4-nitrophenolate, which  
193 can be detected using UV-visible spectrophotometry at 400 nm.<sup>23,24</sup> *Rl*-SRDI565 was grown

194 to mid-logarithmic phase in Y<sub>5%</sub>M and Y<sub>5%</sub>SQ media, and the harvested cells used to prepare  
195 a cell-free lysate containing soluble proteins. Incubation of Y<sub>5%</sub>M and Y<sub>5%</sub>SQ-derived lysates  
196 with PNPSQ both resulted in production of 4-nitrophenolate at similar rates. The activity in  
197 the YSQ-derived lysate was inhibited by the addition of IFG-SQ, an azasugar inhibitor of  
198 SQases that makes key interactions in the active site that mimic those required for substrate  
199 recognition (Figure 4c).<sup>24</sup> The similar levels of activity of SQase in both mannitol and SQ  
200 grown *Rl*-SRDI565 is consistent with the abundance of the putative SQase WP\_017967311.1  
201 detected by proteomic analysis.

202 To further confirm that a sulfo-ED pathway was operative in cells, a targeted  
203 metabolomics approach was used to detect expected intermediates in bacteria grown on  
204 Y<sub>5%</sub>SQ media. Detected intermediates were identified based on their LC-MS/MS retention  
205 time and mass spectra with authentic reference standards of the sulfo-EMP and sulfo-ED  
206 pathway that were synthesized in-house. Sulfogluconate (SG) was synthesized by oxidation  
207 of SQ with iodine<sup>25</sup> (Figures S11 and S12), while SQ, SF, SFP, DHPS, SLA and SL were  
208 prepared as previously reported.<sup>26</sup> *Rl*-SRDI565 was grown to mid-log phase in Y<sub>5%</sub>M or  
209 Y<sub>5%</sub>SQ, metabolically quenched and extracted polar metabolites analyzed by LC/MS-MS.  
210 SQ-grown bacteria contained SQ, SF, SG, SL and DHPS, while SFP and SLA could not be  
211 detected (Figures 5a-e, Figure S14). The detection of SG is characteristic for a sulfo-ED  
212 pathway, and presumably arises from the action of the putative SQ dehydrogenase and SGL  
213 lactonase. The identification of DHPS and SF was unexpected, as these  
214 intermediates/products of the sulfo-EMP pathway.<sup>11</sup> BLAST analysis of the genome of *Rl*-  
215 SRDI565 did not identify putative genes for the sulfo-EMP pathway. SF may therefore be  
216 formed by the action of phosphoglucose isomerase (PGI), while DHPS could be the product  
217 of a promiscuous aldehyde reductase. *Rl*-SRDI565 was unable to utilize DHPS or SL as sole  
218 carbon source in Y<sub>5%</sub> medium, supporting the absence of an alternative pathway of  
219 sulfoglycolysis that utilizes these intermediates. Unexpectedly, cytosolic levels of DHPS  
220 were 20-fold higher than SL, suggesting that cells may lack a membrane transporter to export  
221 accumulated DHPS, in contrast to the SL transporter.

222 NMR and LC-MS/MS analysis of the culture supernatant of both unlabeled and  
223 (<sup>13</sup>C<sub>6</sub>)-labelled SQ-cultivated *Rl*-SRDI565 confirmed that the substrate is almost completely  
224 consumed by the time bacteria reach stationary growth (final concentration of 0.006±0.001  
225 mM compared to 5.0±0.5 mM SQ in starting medium) (Figure S15). Using a highly sensitive  
226 cryoprobe <sup>13</sup>C NMR spectroscopic analysis revealed that both DHPS and SG were present in  
227 culture supernatant of <sup>13</sup>C<sub>6</sub>-SQ-cultivated *Rl*-SRDI565. Quantitative LC-MS/MS analysis

228 showed that consumption of SQ was associated with production of SL ( $5.70\pm0.12$  mM), and  
229 low levels of DHPS ( $0.081\pm0.010$  mM), (SG  $0.172\pm0.006$  mM) and SF ( $0.002\pm0.0001$  mM)  
230 (Table S2). This experiment was repeated to assess the effect of growth of *Rl*-SRDI565 but  
231 using SQGro as carbon source. As noted previously, *Rl*-SRDI565 grows inconsistently on  
232 SQGro and complete consumption of SQGro could not be achieved. However, the results of  
233 partial consumption broadly agreed with the results for growth on SQ, namely that SL is the  
234 major terminal metabolite detected in the culture media, with much lower amounts of SF, SG  
235 and DHPS (Table S2).

236

237

238 **Discussion**

239 We demonstrate here that *Rl*-SRDI565 has a functional sulfo-ED pathway that allows  
240 these bacteria to utilize SQ as their major carbon source. Catabolism of SQ is primarily or  
241 exclusively mediated by a sulfo-ED pathway with production of SL as the major end-product,  
242 similar to the situation in *P. putida* SQ1, the only other experimentally described exemplar of  
243 this pathway.<sup>12</sup> In contrast to *P. putida* SQ1, *Rl*-SRDI565 also produces trace amounts of  
244 DHPS which could reflect the presence of enzymes which exhibit promiscuous activities  
245 similar to those in the conventional sulfo-EMP pathway. This observation is reminiscent of  
246 *Klebsiella* sp. strain ABR11 isolated from soil<sup>27</sup> that is also able to grow on SQ with  
247 production of both SL and DHPS. *Klebsiella* sp. strain ABR11 possesses an NAD<sup>+</sup>-specific  
248 sulfoquinovose-dehydrogenase activity,<sup>28</sup> suggesting it has an operative sulfo-ED pathway.

249 Various bacteria that can metabolize SQ have been isolated from soil including  
250 *Agrobacterium* sp.,<sup>28</sup> *Klebsiella* sp.,<sup>28</sup> and *Flavobacterium* sp.,<sup>29</sup> as well as *P. putida* SQ1,<sup>12</sup>  
251 which was isolated from a freshwater littoral sediment. These bacteria may work  
252 cooperatively with species such as *Paracoccus pantotrophus* NKNCYSA that can convert SL  
253 to mineral sulfur, leading to stoichiometric recovery of sulfite/sulfate.<sup>13</sup> Together these  
254 bacterial communities achieve the complete mineralization of SQ to sulfate, which is  
255 available for use by plants.

256 Proteomic and biochemical evidence suggests that the sulfo-ED pathway is  
257 constitutively expressed in *Rl*-SRDI565, and is subject to only limited up-regulation in the  
258 presence of SQ. As *Rl*-SRDI565 in the soil is likely to be oligotrophic, constitutive  
259 expression of the sulfo-ED pathway may allow simultaneous usage of multiple non-  
260 glycolytic substrates without requirement for significant transcriptional changes. Consistent  
261 with this view, the proteomic abundance of the putative LacI-type regulator  
262 WP\_017967302.1 was unchanged between mannitol and SQ grown *Rl*-SRDI565. The sulfo-  
263 ED operon in *Rl*-SRDI565 differs from that described for *P. putida* SQ1 through the absence  
264 of a putative SQ mutarotase. SQ undergoes mutarotation with a half-life of approximately 6  
265 h, which is much slower than for the glycolytic intermediate Glc-6-P, which has a half-life of  
266 just seconds.<sup>20</sup> Aldose mutarotases are often relatively non-specific and possibly a  
267 constitutive mutarotase not in the sulfo-ED operon expressed by the cell provides this  
268 catalytic capacity. Alternatively, the SQ dehydrogenase may not be stereospecific, with the  
269 ability to act on both anomers of SQ, or even that it acts on  $\alpha$ -SQ (the product released from  
270 SQGro by an SQase) at a high rate such that mutarotation to  $\beta$ -SQ is of insignificant

271 importance. A second difference in the sulfo-ED operon lies in the presence of an ABC  
272 transporter cassette. ABC transporter cassettes are the most common solute transporters, and  
273 can translocate their substrates in either a forward or reverse direction.<sup>30</sup> While we propose  
274 that the ABC transporter cassette operates in the forward direction, based on the presence of a  
275 signal sequence in the putative solute binding domain targeting it to the periplasm, and  
276 consistent with a wide range of sugar import systems, the directionality of transport and thus  
277 the choice of substrate (SQ/SQGro versus SL) may depend on the relative abundance of these  
278 metabolites intra and extracellularly.

279 Sulfoglycolysis in *Rl*-SRDI565 leads to production of pyruvate and the excretion of  
280 the C3-organosulfonate SL (Figure 6). In order to satisfy the demands of the pentose  
281 phosphate pathway and cell wall biogenesis, sulfoglycolytic cells must synthesize glucose-  
282 based metabolites such as glucose-6-phosphate and glucose-1-phosphate. Gluconeogenesis  
283 has been studied in *Rhizobium leguminosarum* strain MNF3841, and operates through a  
284 classical pathway involving fructose bisphosphate aldolase.<sup>31</sup> Action of phosphoglucose  
285 isomerase on SQ might lead to production of SF, thereby explaining the observation of this  
286 metabolite in *Rl*-SRDI565. This is not likely to be consequential, as the reversibility of this  
287 reaction will ultimately allow complete consumption of any SF through isomerization back to  
288 SQ. The formation of DHPS may result from a promiscuous aldehyde reductase. Analysis of  
289 spent culture media reveals that the production of DHPS is minor in terms of total carbon  
290 balance. However, within the cytosol, DHPS accumulates to levels much higher than SL,  
291 presumably because of the absence of a dedicated exporter for the former. Possibly, reduction  
292 of SLA to DHPS is reversible and enables conversion of this metabolite to SL and subsequent  
293 excretion from the cell. The observation of SG, SF and DHPS in the spent culture media at  
294 low levels is suggestive of low levels of leakage of these metabolites from the cell, either  
295 through cell lysis or leaky export systems.

296 Given that SQ contains a significant portion of organic sulfur within plants, the  
297 pathways of SQ catabolism leading to release of its sulfur may be important to enable  
298 recycling of this important macronutrient. Plants can only use sulfate, which is poorly  
299 retained by most soils. Biomineralization of organic sulfur to sulfate is important to allow  
300 plants to access this element. As one of just two known pathways for the catabolism of SQ,  
301 the sulfo-ED pathway is likely to be an important part of environmental breakdown of SQ  
302 and may contribute to the persistence of symbiotic rhizobia within the pedosphere. The  
303 present work lays the groundwork for a more detailed investigation of sulfoglycolysis in a

304 well-characterized bacterium with an established capability for symbiosis of a leguminous  
305 plant host.  
306

307 **Materials and Methods**

308

309 **Reagents**

310 SQ, (<sup>13</sup>C<sub>6</sub>)-SQ, SF, SFP, SLA, SL, and DHPS were synthesized as described previously.<sup>26</sup>

311 IFG-SQ was prepared as described.<sup>24</sup>

312

313 **Bacteria and culture conditions**

314 *Rhizobium leguminosarum* bv. *trifolii* SRDI565 was a gift from Dr Ross Ballard, (South  
315 Australian Research and Development Institute, Adelaide, South Australia). Minimal salts  
316 media consists of 0.5 g·L<sup>-1</sup> K<sub>2</sub>HPO<sub>4</sub>, 0.2 g·L<sup>-1</sup> MgSO<sub>4</sub>, 0.1 g·L<sup>-1</sup> NaCl, 1 M CaCl<sub>2</sub> 3 mL·L<sup>-1</sup>,  
317 adjusted to pH 7.0. YM media consists of minimal salts media plus 1 g·L<sup>-1</sup> yeast extract, 10  
318 g·L<sup>-1</sup> mannitol. Y<sub>5%</sub>M consists of minimal salts media plus 50 mg·L<sup>-1</sup> yeast extract, 5 mM  
319 mannitol. Y<sub>5%</sub>SQ consists of minimal salts media plus 50 mg·L<sup>-1</sup> yeast extract, 5 mM SQ.

320

321 Growth curves were determined in a MicrobeMeter built in-house according to published  
322 plans<sup>32</sup> and blueprints available at <https://humanetechnologies.co.uk/> The MicrobeMeter was  
323 calibrated by performing serial 2-fold dilutions across the detection range of the  
324 MicrobeMeter (0-1023 units), starting with an OD<sub>600</sub> approx. 1 culture of *Rl*-SRDI565. OD<sub>600</sub>  
325 measurements were made with a UV/Vis spectrophotometer and plotted against the reading  
326 of the MicrobeMeter. The data was fit to a polynomial to obtain a calibration curve.

327

328 **Proteomic sample preparation:** Cells were washed 3 times in PBS and collected by  
329 centrifugation at 10,000 x g at 4°C then snap frozen. Frozen whole cell samples were  
330 resuspended in 4% SDS, 100 mM Tris pH 8.0, 20 mM DTT and boiled at 95°C with shaking  
331 at 2000 rpm for 10 minutes. Samples were then clarified by centrifugation at 17,000 x g for  
332 10 minutes, the supernatant collected, and protein concentration determined by bicinchoninic  
333 acid assay (Thermo Scientific Pierce). 100 µg of protein from each sample cleaned up using  
334 SP3 based purification according to previous protocols.<sup>33</sup> Briefly, reduced samples were  
335 cooled and then alkylated with 40 mM 2-chloroacetamide (CAA) for 1 hour at RT in the  
336 dark. The alkylation reactions were then quenched with 40mM DTT for 10 minutes and then  
337 samples precipitated on to SeraMag Speed Beads (GE Healthcare, USA) with ethanol (final  
338 concentration 50% v/v). Samples were shaken for 10 minutes to allow complete precipitation  
339 onto beads and then washed three times with 80% ethanol. The precipitated protein covered  
340 beads were then resuspended in 100mM ammonium bicarbonate containing 2µg trypsin (1/50

341 w/w) and allowed to digest overnight at 37 °C. Upon completion of the digests samples were  
342 spun down at 14000 g for 5 minutes to pellet the beads and the supernatant collected and  
343 desalted using homemade C18 stage tips,<sup>34</sup> then was dried down and stored till analysed by  
344 LC-MS.

345

346 **Proteomics analysis using reversed phase LC-MS:** Purified peptides prepared were re-  
347 suspend in Buffer A\* (2% ACN, 0.1% TFA) and separated using a two-column  
348 chromatography set up composed of a PepMap100 C18 20 mm x 75 µm trap and a PepMap  
349 C18 500 mm x 75 µm analytical column (Thermo Fisher Scientific). Samples were  
350 concentrated onto the trap column at 5 µL/min for 5 minutes and infused an Orbitrap Elite™  
351 (Thermo Fisher Scientific). 120 minute gradients were run altering the buffer composition  
352 from 1% buffer B (80% ACN, 0.1% FA) to 28% B over 90 minutes, then from 28% B to  
353 40% B over 10 minutes, then from 40% B to 100% B over 2 minutes, the composition was  
354 held at 100% B for 3 minutes, and then dropped to 3% B over 5 minutes and held at 3% B for  
355 another 10 minutes. The Elite Orbitrap Mass Spectrometers was operated in a data-dependent  
356 mode automatically switching between the acquisition of a single Orbitrap MS scan (120,000  
357 resolution) and a maximum of 20 MS-MS scans (CID NCE 35, maximum fill time 100 ms,  
358 AGC 1\*10<sup>4</sup>).

359

360 **Mass spectrometry data analysis.** Proteomic comparison of growth with and without  
361 sulfoquinovose was accomplished using MaxQuant (v1.5.5.1).<sup>35</sup> Searches were performed  
362 against *Rhizobium leguminosarum* bv. *trifolii* SRDI565 (NCBI Taxonomy ID: 935549,  
363 downloaded 01-08-2019, 6404 entries) with carbamidomethylation of cysteine set as a fixed  
364 modification. Searches were performed with Trypsin cleavage allowing 2 miscleavage events  
365 and the variable modifications of oxidation of methionine and acetylation of protein N-  
366 termini. The precursor mass tolerance was set to 20 parts-per-million (ppm) for the first  
367 search and 10 ppm for the main search, with a maximum false discovery rate (FDR) of 1.0%  
368 set for protein and peptide identifications. To enhance the identification of peptides between  
369 samples the Match Between Runs option was enabled with a precursor match window set to 2  
370 minutes and an alignment window of 10 minutes. For label-free quantitation, the MaxLFQ  
371 option within MaxQuant<sup>36</sup> was enabled in addition to the re-quantification module. The  
372 resulting peptide outputs were processed within the Perseus (v1.4.0.6)<sup>37</sup> analysis environment  
373 to remove reverse matches and common protein contaminants with missing values imputed.

374 The mass spectrometry proteomics data have been deposited to the ProteomeXchange  
375 Consortium via the PRIDE partner repository with the dataset identifier PXD015822.

376

377 **Chemical synthesis of 6-deoxy-6-sulfo-D-gluconate (SG)**

378 NaOH in methanol (4% w/v, 4 mL) was added dropwise to a stirred solution of  
379 sulfoquinovose (100 mg, 0.410 mmol) and iodine (209 mg, 1.65 mmol) in water (1 mL) and  
380 methanol (4 mL) held at 40 °C. As the sodium hydroxide was added the color of iodine  
381 dissipated. The solvent was evaporated under reduced pressure and the crude residue was  
382 subjected to flash chromatography (EtOAc/MeOH/H<sub>2</sub>O, 4:2:1 to 2:2:1, then water) to give  
383 the 6-deoxy-6-sulfogluconate sodium salt (89.2 mg). An aqueous solution of the sodium salt  
384 was eluted through a column of Amberlite IR120 (H<sup>+</sup> form) resin. The acidic eluate was  
385 collected and concentrated under reduced pressure give SG (71.3 mg, 67%). <sup>1</sup>H NMR (400  
386 MHz, D<sub>2</sub>O): δ 4.23–4.15 (1 H, m, H2), 4.13 (1 H, d, *J* = 3.3 Hz, H3), 4.05 (1 H, t, *J* = 3.2 Hz,  
387 H5), 3.74 (1 H, dd, *J* = 6.5, 3.4 Hz, H4), 3.35 (1 H, d, *J* = 14.6 Hz, H6a), 3.05 (1 H, dd, *J* =  
388 14.6, 9.7 Hz, H6b); <sup>13</sup>C{<sup>1</sup>H} NMR (100 MHz, D<sub>2</sub>O) δ 178.7 (C1), 74.2 (C4), 73.8 (C2), 70.8  
389 (C3), 67.8 (C5), 53.4 (C6); HRMS (ESI<sup>-</sup>) calcd for C<sub>6</sub>H<sub>11</sub>O<sub>9</sub>S [M<sup>-</sup>] 259.0129, found  
390 259.0131.

391

392 **Metabolite analysis of *Rhizobium leguminosarum* cell extracts**

393 **Metabolic quenching and extraction.** *Rl*-SRDI565 was grown on Y<sub>5%</sub>SQ or Y<sub>5%</sub> containing  
394 35 mM glucose to mid-logarithmic phase (approx. 0.15), as calculated based on the OD<sub>600</sub>  
395 measured by Cary 50 UV/visible spectrophotometer, and were rapidly quenched in a  
396 prechilled 15 mL Falcon tube containing phosphate buffered saline (PBS) at 4 °C. Ice-cold  
397 PBS (11 mL) was infused into cell culture media (4 mL). The Falcon tubes were mixed by  
398 inversion and incubated in ice/water slurry for 5 min then were centrifuged at 2000 × *g* at 1  
399 °C for 10 min. The supernatant was removed by aspiration and cell pellets were washed twice  
400 with 1 mL of ice-cold PBS (with resuspension each time) and transferred into 1.5 mL  
401 Eppendorf tubes. Cells were pelleted by centrifugation at 14000 rpm and residual solvent was  
402 carefully removed. Cell pellets were stored at -80°C until extraction. Cells were extracted in  
403 200 μL of extraction solution (methanol/water, 3:1 v/v) containing an internal standard, 5 μM  
404 <sup>13</sup>C<sub>4</sub>-aspartate (Cambridge Isotopes), and subjected to 10 freeze-thaw cycles to facilitate cell  
405 lysis (30 s in liquid nitrogen, followed by 30 s in dry ice/ethanol bath). Debris was pelleted  
406 by centrifugation at 14000 rpm, 5 min, 1°C and cell lysate was transferred into a HPLC vial  
407 insert for LC/MS analysis.

408 **LC/MS analysis and identification of sulfonate metabolites.** Separation and detection of  
409 polar metabolites was performed using an Agilent Technologies 1200 series high  
410 performance liquid chromatography (HPLC) coupled to a quadrupole time-of-flight mass  
411 spectrometer (6545 QTOF, Agilent Technologies) using a method modified from  
412 Masukagami *et al.*<sup>38</sup> Metabolite extracts were transferred into 2 mL auto sampler vials with  
413 glass inserts and placed in the auto sampler kept at 4 °C prior to analysis. Metabolite  
414 separation was performed by injecting 7 µL of the extract into a SeQuant® ZIC-pHILIC  
415 PEEK coated column (150 mm × 4.6 mm, 5 µm polymer, Merck Millipore) maintained at  
416 25°C, with a gradient of solvent A (20 mM ammonium carbonate, pH 9.0, Sigma-Aldrich)  
417 and solvent B (100% acetonitrile, Hypergrade for LCMS LiChrosolv, Merck) at a flow rate  
418 of 0.3 mL/min. A 33.0 min gradient was setup with time (*t*) = 0 min, 80% B; *t* = 0.5 min,  
419 80% B; *t* = 15.5 min, 50% B; *t* = 17.5 min, 30% B; *t* = 18.5 min, 5% B; *t* = 21.0 min, 5% B; *t*  
420 = 23.0 min, 80% B.

421 The LC flow was directed into an electrospray ionization (ESI) source with a capillary  
422 voltage of 2500 V operating in negative ionization mode. Drying nitrogen gas flow was set to  
423 10 L/min, sheath gas temperature and nebulizer pressure were set to 300 °C and 20 psi,  
424 respectively. The voltages of fragmentor and skimmer were set at 125 V and 45 V,  
425 respectively. Data was acquired in MS and MS/MS mode, with a scan range of 60 to 1700  
426 *m/z* and 100 to 1700 *m/z* respectively, at a rate of 1.5 spectra/sec. MS/MS acquisition was  
427 performed with four collision energies (0, 10, 20 and 40 V). The mass spectrometer was  
428 calibrated in negative mode prior to data acquisition and mass accuracy during runs was  
429 ensured by a continuous infusion of reference mass solution at a flow rate of 0.06 mL/min  
430 (API-TOF Reference Mass Solution Kit, Agilent Technologies). Data quality was ensured by  
431 multiple injections of standards (with 1.5 µM concentration each) and pooled biological  
432 sample (a composite of cell extracts) used to monitor the instrument performance. Samples  
433 were randomized prior to metabolite extraction and LC/MS analysis.

434 **Standard preparation.** Standards of selected metabolites (Supplementary Table 1) were  
435 prepared at 10 µM in 80% acetonitrile (Hypergrade for LCMS LiChrosolv, Merck) and  
436 injected separately into a column connected to mass spectrometer interface. Retention time  
437 and detected molecular ion were used to create a targeted MS/MS acquisition method. The  
438 spectra, mass to charge (*m/z*) and retention time (RT) were imported into a personal  
439 compound database and library (PCDL Manager, version B.07.00, Agilent Technologies)  
440 used in data processing workflow.

441 **Data analysis.** Data were analysed using MassHunter Qualitative and Quantitative Analysis  
442 software (version B.07.00, Agilent Technologies). Identification of metabolites was  
443 performed in accordance with metabolite identification (Metabolomics Standard Initiative,  
444 MSI) level 1 based on the retention time and molecular masses matching to authentic  
445 standards included in the personal database and library. Peak integration was performed in  
446 MassHunter quantitative software (version B.07.00, Agilent Technologies) on the spectra  
447 from identified metabolites.

448

449 **Cloning, expression and kinetic analysis of *Rl-SRD1565* sulfoquinovosidase (*RlSQase\**)**

450 The gene sequence coding for *RlSQase\** SERp mutant was synthesised with codon  
451 optimisation for expression in *E. coli* and was cloned within a pET-28a(+) vector with C-  
452 terminal His-tag through GenScript. The plasmid His<sub>6</sub>-*RlSQase\**-pET-28a(+) containing the  
453 gene for target *RlSQase\** was transformed into *E. coli* BL21(DE3) cells for protein  
454 expression. Pre-cultures were grown in LB-medium (5 mL) containing 30 µg/mL for 18 h at  
455 37 °C, 200 rpm. Cultures (1 L LB-medium supplemented with kanamycin 30 µg/mL) were  
456 inoculated with the pre-culture (5 mL) and incubated at 37 °C, 200 rpm until an OD<sub>600</sub> of 0.6-  
457 0.8 was achieved. Protein expression was induced by addition of IPTG (1 mM) and shaking  
458 was continued overnight (20-22 h) at 18 °C, 200 rpm. The cells were harvested by  
459 centrifugation (5000 rpm, 4 °C, 20 min), resuspended in 50 mM Tris, 300 mM NaCl pH 7.5  
460 buffer and were subjected to further cell lysis. Cells were disrupted using French press under  
461 20 k Psi pressure and the lysate was centrifuged at 50,000 g for 30 min.

462 The N-terminal His<sub>6</sub>-tagged protein was purified by immobilized metal ion affinity  
463 chromatography, followed by size exclusion chromatography (SEC) (Figure S10a). The  
464 lysate was loaded onto a pre-equilibrated Ni-NTA column, followed by washing with load  
465 buffer (50 mM Tris-HCl, 300 mM NaCl, 30 mM imidazole pH 7.5). The bound protein was  
466 eluted using a linear gradient with buffer containing 500 mM imidazole. Protein containing  
467 fractions were pooled, concentrated and loaded onto a HiLoad 16/600 Superdex 200 gel  
468 filtration column pre-equilibrated with 50 mM Tris-HCl, 300 mM NaCl pH 7.5 buffer. The  
469 protein was concentrated to a final concentration of 60 mg mL<sup>-1</sup> using a Vivaspin® 6 with a  
470 300 kDa MW cut-off membrane for characterization and enzyme assays.

471

472 **SEC-MALS analysis**

473 Experiments were conducted on a system comprising a Wyatt HELEOS-II multi-angle light  
474 scattering detector and a Wyatt rEX refractive index detector linked to a Shimadzu HPLC

475 system (SPD-20A UV detector, LC20-AD isocratic pump system, DGU-20A3 degasser and  
476 SIL-20A autosampler). Experiments were conducted at room temperature ( $20 \pm 2^\circ\text{C}$ ).  
477 Solvents were filtered through a  $0.2 \mu\text{m}$  filter prior to use and a  $0.1 \mu\text{m}$  filter was present in  
478 the flow path. The column was equilibrated with at least 2 column volumes of buffer (50 mM  
479 Tris, 300 mM NaCl pH 7.5) before use and buffer was infused at the working flow rate until  
480 baselines for UV, light scattering and refractive index detectors were all stable. The sample  
481 injection volume was 100  $\mu\text{L}$  *RlSQase*\* at 6 mg/mL in 50 mM Tris buffer, 300 mM NaCl pH  
482 7.5. Shimadzu LC Solutions software was used to control the HPLC and Astra V software for  
483 the HELEOS-II and rEX detectors (Figure S10b). The Astra data collection was 1 min shorter  
484 than the LC solutions run to maintain synchronisation. Blank buffer injections were used as  
485 appropriate to check for carry-over between sample runs. Data were analysed using the Astra  
486 V software. Molar masses were estimated using the Zimm fit method with degree 1. A value  
487 of 0.158 was used for protein refractive index increment ( $\text{dn/dc}$ ).

488

#### 489 **Enzyme kinetics of *RlSQase***

490 **Michaelis Menten plot.** Kinetic analysis of *RlSQase*\* was performed using PNPSQ as  
491 substrate, using a UV/visible spectrophotometer to measure the release of the 4-  
492 nitrophenolate ( $\lambda = 348 \text{ nm}$ ). Assays were carried out in 50 mM sodium phosphate, 150 mM  
493 NaCl, pH 7.2 at  $30^\circ\text{C}$  using 212 nM *RlSQase*\* at substrate concentrations ranging from 0.05  
494  $\mu\text{M}$  to 4 mM. Using the extinction coefficient for 4-nitrophenolate of  $5.125 \text{ mM}^{-1} \text{ cm}^{-1}$ ,  
495 kinetic parameters were calculated using Prism.

496 **pH profile.** For the determination of pH profile, specific activities of *RlSQase*\* were  
497 monitored by measuring absorbance changes at  $\lambda = 348 \text{ nm}$  in the presence of the following  
498 buffers: sodium acetate buffer (pH 5.6, sodium phosphate buffer (pH 6.0–8.5), and glycine  
499 NaOH buffer (pH 8.8–9.2). The assays were performed at  $30^\circ\text{C}$  in duplicates and specific  
500 activities determined using extinction coefficient of PNP at isobestic point (348 nM) as  $5.125$   
501  $\text{mM}^{-1} \text{ cm}^{-1}$  (Supplementary Figure Sx). One unit of SQase activity is defined as the amount  
502 of protein that releases 1  $\mu\text{mol}$  PNP per minute.

503

#### 504 **Detection of SQase activity in cell lysates**

505 *Rl-SRDI565* was grown in 50 mL Y<sub>5%</sub>M and Y<sub>5%</sub>SQ media at  $30^\circ\text{C}$  to mid log phase,  
506 approximately  $\text{OD}_{600} = 0.2$ , measured using a Varian Cary50 UV/visible spectrophotometer.  
507 Cells were harvested by adding 3 $\times$  volume of ice-cold PBS to metabolically quench the  
508 samples then centrifuged at 2000 g,  $4^\circ\text{C}$  for 10 min. The supernatant was discarded and the

509 cells were washed 3 times with ice-cold PBS, with each wash involving resuspension and  
510 centrifugation at 2000 g, 4 °C for 10 min. The cells were collected once more by  
511 centrifugation at 10,000 g, 4 °C, for 1 min then snap frozen in liquid nitrogen and stored at -  
512 80 °C.

513 Cells were lysed by addition of 1000 µL pre-chilled PBS, 1 µL RNaseA, 1 µL DNase,  
514 1 µL 100 mg·mL<sup>-1</sup> hen egg white lysozyme (Sigma), and a 1× final concentration of  
515 cOmplete EDTA-free protease inhibitor cocktail (Roche) to the cell pellet. The cells were  
516 gently resuspended and mixed at 4 °C for 10 min. The suspension was placed on ice and  
517 irradiated with a Sonoplus HD3200 MS 73 sonicator probe (Bandelin) at a frequency of 20  
518 kHz, 20% amplitude, pulse 2s on 8s off, repeated for a total time of the sonication to 150 s,  
519 then incubated on ice for 5 min. The suspension was clarified by centrifuging at 14,000 g, 4  
520 □ for 1 min and the supernatant was filtered through a Nanosep mini centrifugal spin column  
521 with a 0.2 µm filter (Pall) into a 1.5mL Eppendorf tubes and stored at 4 °C. Protein  
522 concentration was determined using a BCA assay.

523 SQase activity was measured in triplicate using PNPSQ and an Agilent Cary UV  
524 Workstation (G5191-64000) at 30□. Reactions contained buffer consisted of 50 mM NaPi  
525 and 150 mM NaCl, pH=7.4, and 2.5 mM PNPSQ. Reactions were initiated by addition of  
526 SQ- or mannitol-derived lysate to a final concentration of 43.7 µg·mL<sup>-1</sup> protein, and  
527 absorbance was monitored at 400 nm for 3 h. After 3 h, IFGSQ was added to a final  
528 concentration of 6.25 mM to the SQ-lysate sample, and absorption monitored for 3 h.

529

### 530 **Quantitation of metabolite levels in spent culture media**

531 The metabolites (DHPS, SF, SQ, SL and SG) present in spent culture media were quantified  
532 against standard solutions of pure metabolites by HPLC-ESI-MS/MS. Quantification was  
533 done with the aid of calibration curves generated by dissolving the pure standards in spent  
534 media from *Rl*-SRDI565 grown on Y<sub>5%</sub>M. Spiked spent media was diluted 100-fold with  
535 water and then analysed by LC-MS/MS with α-MeSQ as internal standard. For experimental  
536 determination of metabolites, spent culture media from *Rl*-SRDI565 grown in Y<sub>5%</sub>SQ or  
537 Y<sub>5%</sub>SQGro were diluted 100-fold with water and analysed by LC-MS/MS with α-MeSQ as  
538 internal standard.

539 HPLC-ESI-MS/MS analysis was performed using a TSQ Altis triple quadrupole mass  
540 spectrometer (Thermo Fisher Scientific) coupled with a Vanquish Horizon UHPLC system  
541 (Thermo Fisher Scientific). The column was a ZIC-HILIC column (5 µm, 50 × 2.1 mm;

542 Merck). The HPLC conditions were: from 90% B to 40% B over 15 min; then 40% B for 5  
543 min; back to 90% B over 1 min (solvent A: 20 mM NH<sub>4</sub>OAc in 1% acetonitrile; solvent B:  
544 acetonitrile); flow rate, 0.30 ml min<sup>-1</sup>; injection volume, 1  $\mu$ l. The mass spectrometer was  
545 operated in negative ionization mode. Quantitation was done using the MS/MS selected  
546 reaction monitoring (SRM) mode using Thermo Scientific XCalibur software and normalized  
547 with respect to the internal standard,  $\alpha$ -MeSQ. Prior to analysis, for each analyte, the  
548 sensitivity for each SRM-MS/MS transition was optimized.

549 DHPS: ESI-MS/MS *m/z* of [M-H]<sup>-</sup> 155, product ions 137, 95; retention time: 4.91 min

550  $\alpha$ -MeSQ (internal standard): ESI-MS/MS *m/z* of [M-H]<sup>-</sup> 257, product ions 166, 81;  
551 retention time: 6.31 min

552 SF: ESI-MS/MS *m/z* of [M-H]<sup>-</sup> 243, product ions 207, 153; retention time: 6.81 min

553 SQ: ESI-MS/MS *m/z* of [M-H]<sup>-</sup> 243, product ions 183, 123; retention time: 7.58 and 7.89  
554 min for  $\alpha$  /  $\beta$

555 SL: ESI-MS/MS *m/z* of [M-H]<sup>-</sup> 169, product ions 107, 71; retention time: 9.26 min

556 SG: ESI-MS/MS *m/z* of [M-H]<sup>-</sup> 259, product ions 241, 161; retention time: 9.66 min

557 SQGro: ESI-MS/MS *m/z* of [M-H]<sup>-</sup> 317, product ions 225, 165; retention time: 7.15 min

558

## 559 Acknowledgements

560

561 This work was supported by grants from the Australian Research Council (DP180101957),  
562 the National Health and Medical Research Council of Australia (APP1100164,  
563 GNT1139549) and the Leverhulme Trust; support from The Walter and Eliza Hall Institute of  
564 Medical Research, the Australian Cancer Research Fund, and a Victorian State Government  
565 Operational Infrastructure support grant. MJM is an NHMRC Principal Research Fellow,  
566 G.J.D. is a Royal Society Ken Murray Research Fellow. JL is supported by a PhD scholarship  
567 from the Chinese Scholarship Council. We thank Humane Technologies for support with the  
568 MicrobeMeter, the Melbourne Mass Spectrometry and Proteomics Facility of the Bio21  
569 Institute at the University of Melbourne, Palika Abayakoon and Janice Mui for reagents, and  
570 Dr Shuai Nie, Yunyang Zhang and Alex Chen (Thermo Fisher) for technical support. Thermo  
571 Fisher Scientific Australia are acknowledged for access to the TSQ Altis triple quadrupole  
572 mass spectrometer.

573

574

575 **References**

576

- 577 1. Hu ZY, Zhao, F.J. & McGrath, S.P. Sulphur fractionation in calcareous soils and  
578 bioavailability to plants. *Plant Soil* **268**, 103-109 (2005).
- 579 2. Wilhelm Scherer H. Sulfur in soils. *J. Plant Nutr. Soil Sci.* **172**, 326-335 (2009).
- 580 3. Scherer HW. Sulphur in crop production — invited paper. *Eur. J. Agronomy* **14**, 81-  
581 111 (2001).
- 582 4. Tabatabai MA. Importance of Sulphur in Crop Production. *Biogeochemistry* **1**, 45-62  
583 (1984).
- 584 5. Kertesz MA, Mirleau P. The role of soil microbes in plant sulphur nutrition. *J. Exp.*  
585 *Bot.* **55**, 1939-1945 (2004).
- 586 6. Harwood JL, Nicholls RG. The plant sulpholipid - a major component of the sulphur  
587 cycle. *Biochem. Soc. Trans.* **7**, 440-447 (1979).
- 588 7. Goss R, Nerlich J, Lepetit B, Schaller S, Vieler A, Wilhelm C. The lipid dependence  
589 of diadinoxanthin de-epoxidation presents new evidence for a macrodomain  
590 organization of the diatom thylakoid membrane. *J. Plant Physiol.* **166**, 1839-1854  
591 (2009).
- 592 8. Strickland TC, Fitzgerald JW. Mineralization of sulphur in sulfoquinovose by forest  
593 soils. *Soil Biol. Biochem.* **15**, 347-349 (1983).
- 594 9. Kertesz MA. Riding the sulfur cycle - metabolism of sulfonates and sulfate esters in  
595 Gram-negative bacteria. *FEMS Microbiol. Rev.* **24**, 135-175 (2000).
- 596 10. Goddard-Borger ED, Williams SJ. Sulfoquinovose in the biosphere: occurrence,  
597 metabolism and functions. *Biochem. J.* **474**, 827-849 (2017).
- 598 11. Denger K, Weiss M, Felix AK, Schneider A, Mayer C, Spitteler D, Huhn T, Cook  
599 AM, Schleheck D. Sulphoglycolysis in *Escherichia coli* K-12 closes a gap in the  
600 biogeochemical sulphur cycle. *Nature* **507**, 114-117 (2014).
- 601 12. Felix AK, Spitteler D, Klebensberger J, Schleheck D. Entner-Doudoroff pathway for  
602 sulfoquinovose degradation in *Pseudomonas putida* SQ1. *Proc. Natl. Acad. Sci. USA*  
603 **112**, E4298-4305 (2015).
- 604 13. Denger K, Huhn T, Hollemeyer K, Schleheck D, Cook AM. Sulfoquinovose degraded  
605 by pure cultures of bacteria with release of C<sub>3</sub>-organosulfonates: complete  
606 degradation in two-member communities. *FEMS Microbiol. Lett.* **328**, 39-45 (2012).
- 607 14. Drew EA, Ballard RA. Improving N<sub>2</sub> fixation from the plant down: Compatibility of  
608 *Trifolium subterraneum* L. cultivars with soil rhizobia can influence symbiotic  
609 performance. *Plant Soil* **327**, 261-277 (2010).
- 610 15. Melino VJ, Drew EA, Ballard RA, Reeve WG, Thomson G, White RG, O'Hara GW.  
611 Identifying abnormalities in symbiotic development between *Trifolium* spp. and  
612 *Rhizobium leguminosarum* bv. trifolii leading to sub-optimal and ineffective nodule  
613 phenotypes. *Ann. Bot.* **110**, 1559-1572 (2012).
- 614 16. Reeve W, Drew E, Ballard R, Melino V, Tian R, De Meyer S, Brau L, Ninawi M,  
615 Teshima H, Goodwin L, Chain P, Liolios K, Pati A, Mavromatis K, Ivanova N,  
616 Markowitz V, Woyke T, Kyrpides N. Genome sequence of the clover-nodulating  
617 *Rhizobium leguminosarum* bv. trifolii strain SRDI565. *Stand. Genomic Sci.* **9**, 220-  
618 231 (2013).
- 619 17. Udvardi M, Poole PS. Transport and metabolism in legume-rhizobia symbioses.  
620 *Annu. Rev. Plant Biol.* **64**, 781-805 (2013).
- 621 18. Poole P, Ramachandran V, Terpolilli J. Rhizobia: from saprophytes to  
622 endosymbionts. *Nat. Rev. Microbiol.* **16**, 291-303 (2018).

623 19. Stowers MD. Carbon metabolism in Rhizobium species. *Annu. Rev. Microbiol.* **39**,  
624 89-108 (1985).

625 20. Abayakoon P, Lingford JP, Jin Y, Bengt C, Davies GJ, Yao S, Goddard-Borger ED,  
626 Williams SJ. Discovery and characterization of a sulfoquinovose mutarotase using  
627 kinetic analysis at equilibrium by exchange spectroscopy. *Biochem. J.* **475**, 1371-  
628 1383 (2018).

629 21. Bergersen FJ. The growth of rhizobium in synthetic media. *Aust. J. Biol. Sci.* **14**, 349-  
630 360 (1961).

631 22. Goldschmidt L, Cooper DR, Derewenda ZS, Eisenberg D. Toward rational protein  
632 crystallization: A Web server for the design of crystallizable protein variants. *Protein*  
633 *Sci.* **16**, 1569-1576 (2007).

634 23. Speciale G, Jin Y, Davies GJ, Williams SJ, Goddard-Borger ED. YihQ is a  
635 sulfoquinovosidase that cleaves sulfoquinovosyl diacylglyceride sulfolipids. *Nat.*  
636 *Chem. Biol.* **12**, 215-217 (2016).

637 24. Abayakoon P, Jin Y, Lingford JP, Petricevic M, John A, Ryan E, Wai-Ying Mui J,  
638 Pires DEV, Ascher DB, Davies GJ, Goddard-Borger ED, Williams SJ. Structural and  
639 Biochemical Insights into the Function and Evolution of Sulfoquinovosidases. *ACS*  
640 *Cent. Sci.* **4**, 1266-1273 (2018).

641 25. Roy AB, Hewlins MJE. Sulfoquinovose and its aldonic acid: their preparation and  
642 oxidation to 2-sulfoacetaldehyde by periodate. *Carbohydr. Res.* **302**, 113-117 (1997).

643 26. Abayakoon P, Epa R, Petricevic M, Bengt C, Mui JWY, van der Peet PL, Zhang Y,  
644 Lingford JP, White JM, Goddard-Borger ED, Williams SJ. Comprehensive synthesis  
645 of substrates, intermediates and products of the sulfoglycolytic Embden-Meyerhoff-  
646 Parnas pathway. *J. Org. Chem.* **84**, 2910-2910 (2019).

647 27. Roy AB, Ellis AJ, White GF, Harwood JL. Microbial degradation of the plant  
648 sulpholipid. *Biochem. Soc. Trans.* **28**, 781-783 (2000).

649 28. Roy AB, Hewlins MJ, Ellis AJ, Harwood JL, White GF. Glycolytic breakdown of  
650 sulfoquinovose in bacteria: a missing link in the sulfur cycle. *Appl. Environ.*  
651 *Microbiol.* **69**, 6434-6441 (2003).

652 29. Martelli HL, Benson AA. Sulfocarbohydrate metabolism. I. Bacterial production and  
653 utilization of sulfoacetate. *Biochim. Biophys. Acta* **93**, 169-171 (1964).

654 30. Davidson AL, Dassa E, Orelle C, Chen J. Structure, Function, and Evolution of  
655 Bacterial ATP-Binding Cassette Systems. *Microbiol. Mol. Biol. Rev.* **72**, 317-364  
656 (2008).

657 31. McKay IA, Glenn AR, Dilworth MJ. Gluconeogenesis in *Rhizobium leguminosarum*  
658 MNF3841. *Microbiology* **131**, 2067-2073 (1985).

659 32. Sasidharan K, Martinez-Vernon AS, Chen J, Fu T, Soyer OS. A low-cost DIY device  
660 for high resolution, continuous measurement of microbial growth dynamics. *bioRxiv*,  
661 407742 (2018).

662 33. Hughes CS, Moggridge S, Müller T, Sorensen PH, Morin GB, Krijgsveld J. Single-  
663 pot, solid-phase-enhanced sample preparation for proteomics experiments. *Nat.*  
664 *Protoc.* **14**, 68-85 (2019).

665 34. Rappaport J, Mann M, Ishihama Y. Protocol for micro-purification, enrichment, pre-  
666 fractionation and storage of peptides for proteomics using StageTips. *Nat. Protoc.* **2**,  
667 1896-1906 (2007).

668 35. Cox J, Mann M. MaxQuant enables high peptide identification rates, individualized  
669 p.p.b.-range mass accuracies and proteome-wide protein quantification. *Nat.*  
670 *Biotechnol.* **26**, 1367-1372 (2008).

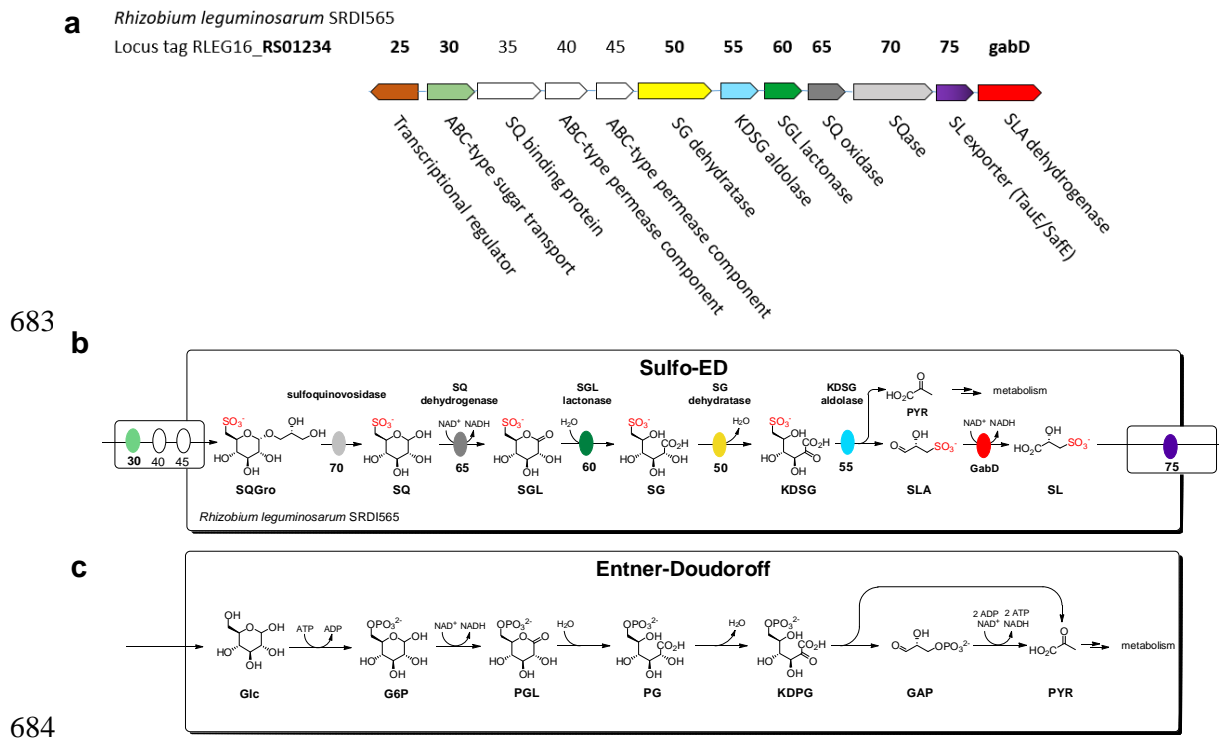
671 36. Cox J, Hein MY, Luber CA, Paron I, Nagaraj N, Mann M. Accurate Proteome-wide  
672 Label-free Quantification by Delayed Normalization and Maximal Peptide Ratio  
673 Extraction, Termed MaxLFQ. *Mol. Cell. Proteomics* **13**, 2513 (2014).

674 37. Tyanova S, Temu T, Sinitcyn P, Carlson A, Hein MY, Geiger T, Mann M, Cox J. The  
675 Perseus computational platform for comprehensive analysis of (prote)omics data. *Nat.*  
676 *Methods* **13**, 731 (2016).

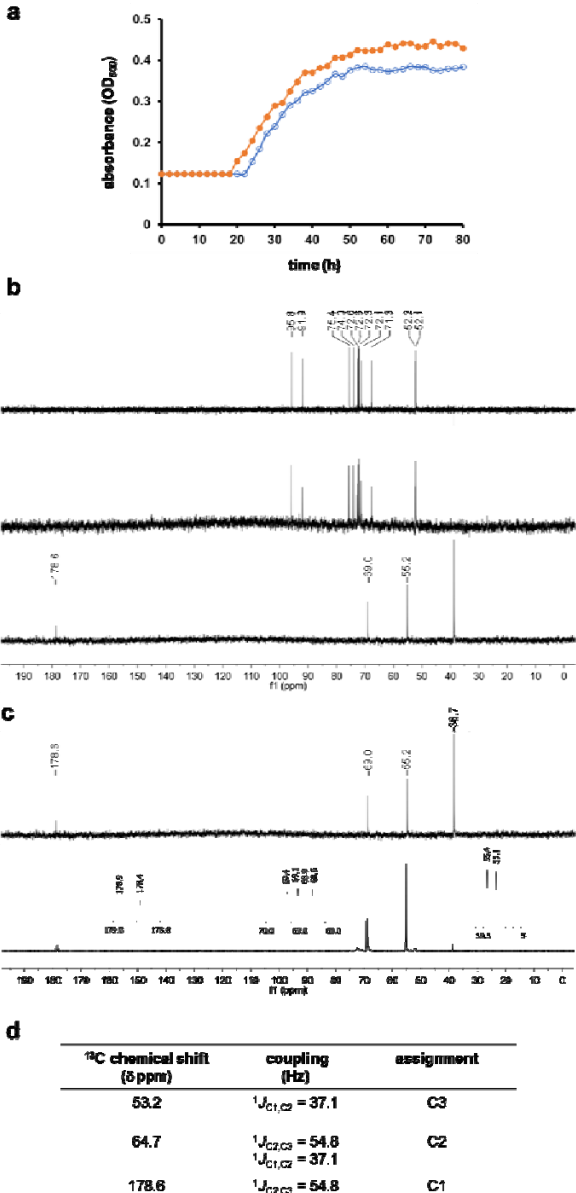
677 38. Masukagami Y, Nijagal B, Mahdizadeh S, Tseng CW, Dayalan S, Tivendale KA,  
678 Markham PF, Browning GF, Sansom FM. A combined metabolomic and  
679 bioinformatic approach to investigate the function of transport proteins of the  
680 important pathogen *Mycoplasma bovis*. *Vet. Microbiol.* **234**, 8-16 (2019).

681

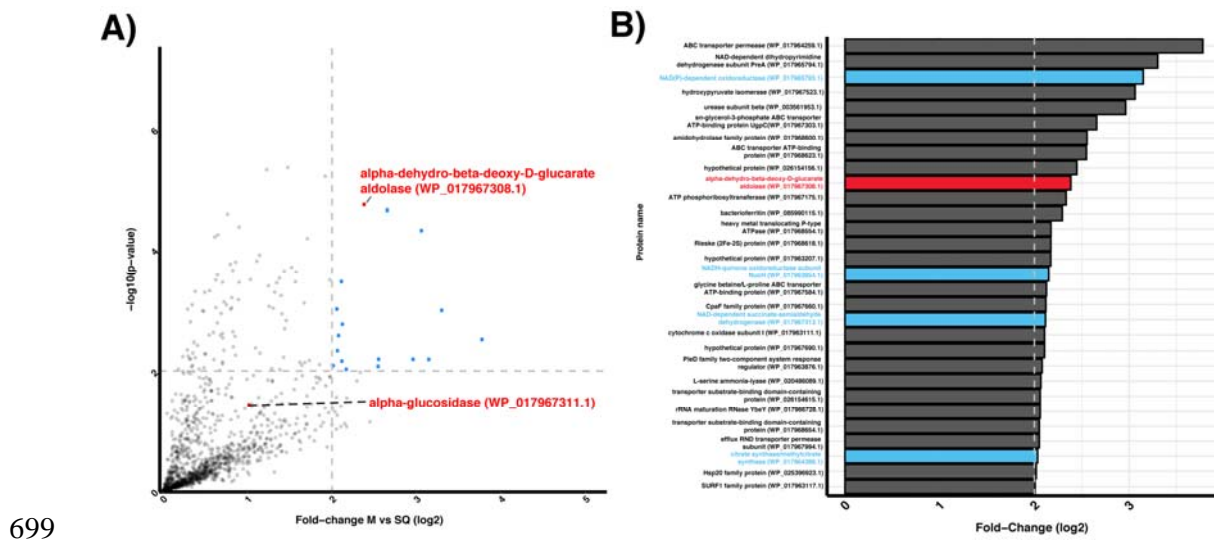
682



686 **Figure 1: Proposed sulfoglycolytic Entner-Doudoroff (sulfo-ED) pathway in *Rhizobium***  
687 ***leguminosarum* bv. *trifolii* SRDI565.** (a) Operon encoding sulfo-ED pathway. (b) Proposed  
688 sulfo-ED pathway. (c) Comparison with the Entner-Doudoroff pathway.



689 **Figure 2: Growth of *Rhizobium leguminosarum* bv. *trifolii* SRDI565 on SQ produces SL**  
 690 **as the major terminal metabolite.** a) Growth of *Rl*-SRDI565 on 5% yeast extract media  
 691 containing 5 mM SQ (●) or 5 mM mannitol (○). This data is representative of 2 independent  
 692 experiments. b)  $^{13}\text{C}$  NMR (126 MHz) spectra of (top) SQ, (middle) 5 mM SQ in 5% yeast  
 693 extract media and (bottom) spent culture media from growth of *Rl*-SRDI565 on 5 mM SQ. c)  
 694  $^{13}\text{C}$  NMR (126 MHz) spectrum of spent culture media from growth of *Rl*-SRDI565 on 5 mM  
 695 ( $^{13}\text{C}_6$ )-SQ. The signal at  $\delta$  38.7 ppm is present in control experiments of *Rl*-SRDI565 grown  
 696 on mannitol and is believed to derive from yeast extract. d) Tabulated  $^{13}\text{C}$  NMR (126 MHz)  
 697 data for  $^{13}\text{C}_3$ -SL from (c). All samples contain 10%  $\text{D}_2\text{O}$ , added to allow frequency lock.



699

700

701 **Figure 3: Proteomic analysis of *Rhizobium leguminosarum* SRDI565 growth in**  
702 **sulfoquinovose.** Quantitative proteomics was undertaken to identify proteins associated with

703 sulfoquinovose catabolism versus mannitol. A) Examination of proteins observed to increase

704 in abundance greater than four-fold revealed 30 proteins including alpha-dehydro-beta-

705 deoxy-D-glucarate aldolase (WP\_017967308.1). B) Growth in sulfoquinovose leads to the

706 increase of multiple proteins associated with the TCA cycle including NAD(P)-dependent

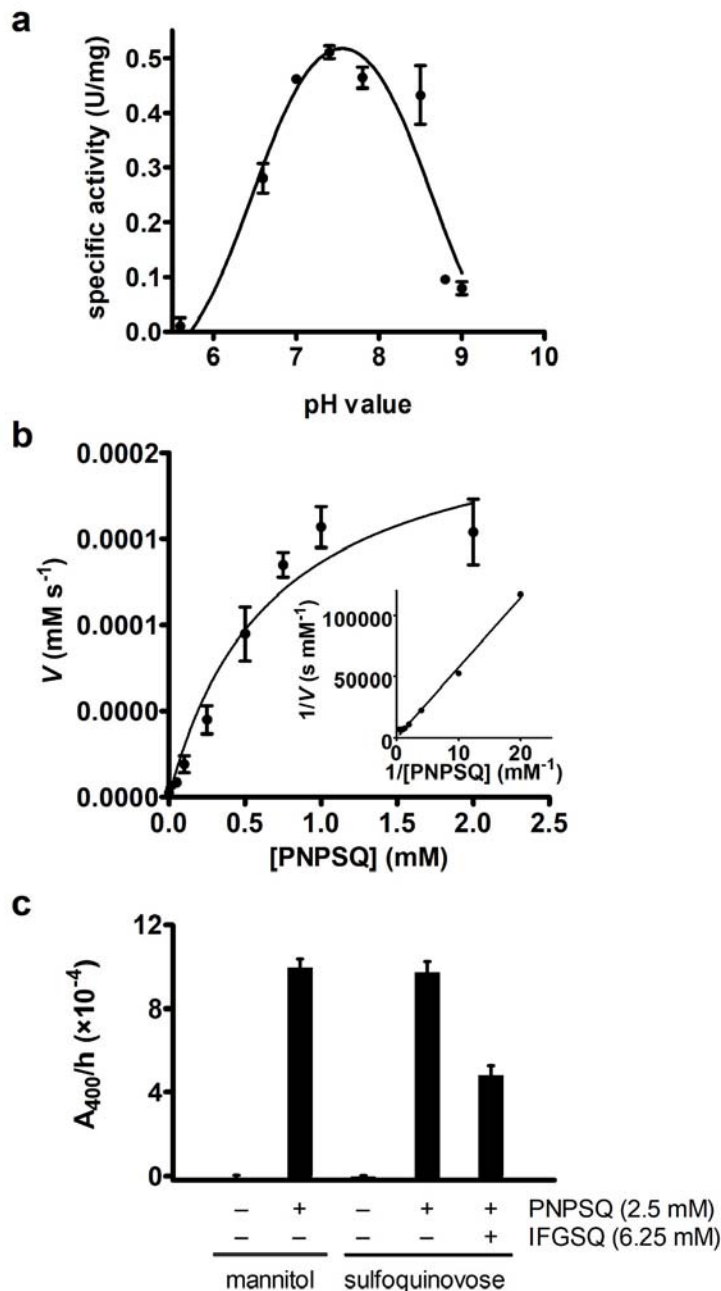
707 oxidoreductase (WP\_017965793.1), NADH-quinone oxidoreductase subunit NuoH

708 (WP\_017963854.1), NAD-dependent succinate-semialdehyde dehydrogenase

709 (WP\_017967313.1) and citrate synthase/methylcitrate synthase (WP\_017964386.1)

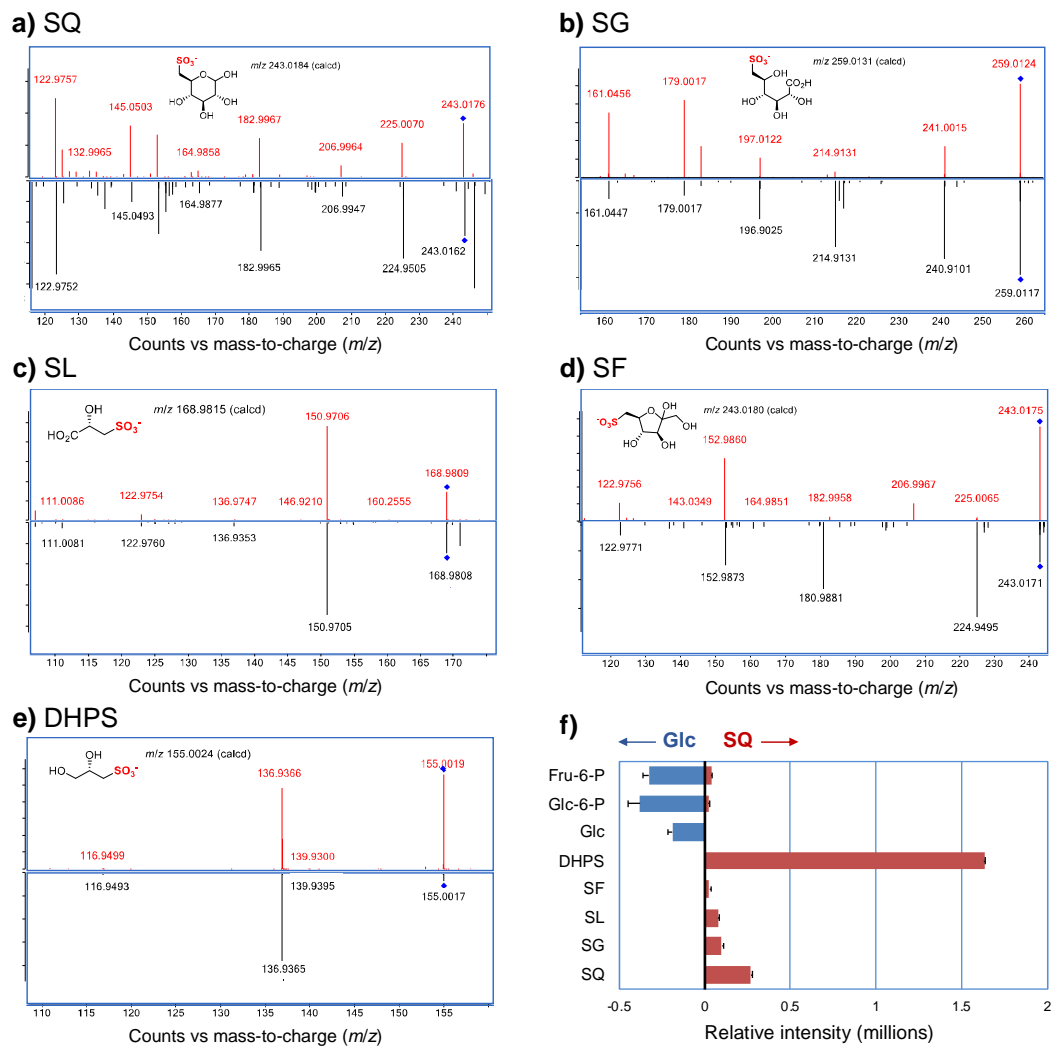
710 highlighted in blue.

711



712

713 **Figure 4: *Rhizobium leguminosarum* SRDI565 produces a functional sulfoquinovosidase**  
714 **that can be detected in cell lysates.** a) pH profile of *RlSQase\**. Specific activities were  
715 determined for hydrolysis of PNPSQ. b) Michaelis-Menten plot of kinetic parameters for  
716 *RlSQase\** for hydrolysis of PNPSQ. c) Analysis of sulfoquinovosidase activity of *Rl-*  
717 SRDI565 lysate grown on sulfoquinovose and mannitol. Cell lysates of soluble proteins  
718 derived from growth on SQ or mannitol was standardized for equal protein and SQase  
719 activity measured using the chromogenic substrate PNPSQ. SQase activity was confirmed by  
720 inhibition by the azasugar inhibitor SGIFG. Error bars denote standard error of the mean.



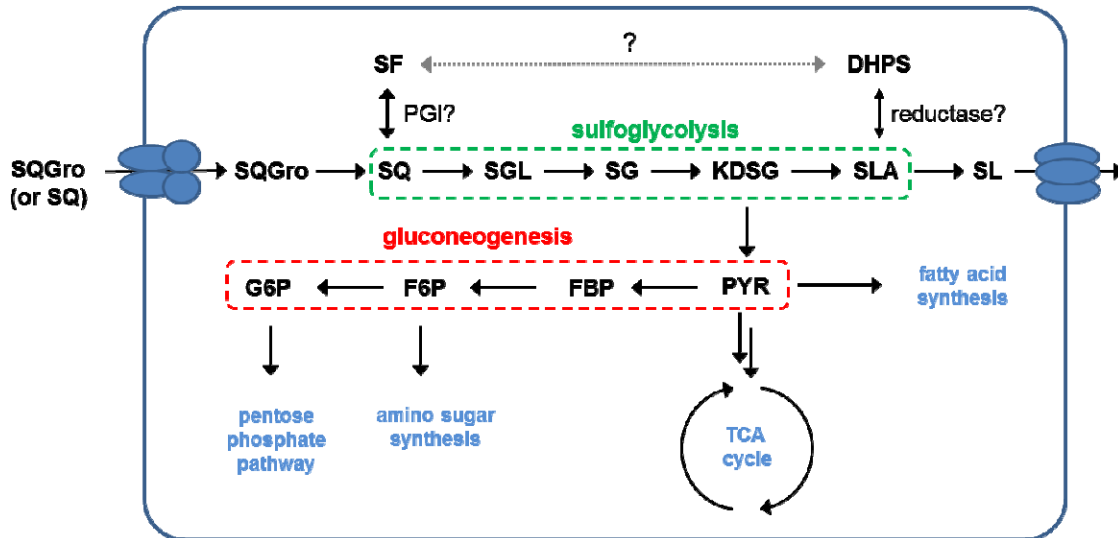
721

722

723 **Figure 5: Detection of sulfoglycolytic intermediates and end-products in cytosolic**  
 724 **extracts of *Rl-SRDI565*.** *Rl-SRDI565* was grown on Y<sub>5%</sub>SQ media and metabolically-  
 725 quenched by rapid cooling to 4 C, followed by extraction of cellular metabolites and lc/ms  
 726 analysis. Detection of sulfoglycolytic and glycolytic/neoglucogenic intermediates A) SQ, B)  
 727 SG, C) SL, D) SF, E) DHPS. In each case the upper panel corresponds to the collision-  
 728 induced dissociation mass spectrum of chemically-synthesized standard, while the lower  
 729 panel is the equivalent mass spectrum for the metabolite identified in the cytosolic extract. F)  
 730 Relative mass spectrometric intensities of metabolites from cells grown on Glc or SQ.

731

732



733

734 **Figure 6: Proposed pathway for SQ metabolism in *Rhizobium leguminosarum* SRDI565.**

735